Metformin Hydrochloride and Sitagliptin Phosphate Fixed Dose Combination Product Prepared Using Melt Granulation Continuous Processing Technology

Kelleher, J., Madi, A., Gilvary, G. C., Tian, J., Li, S., Almajaan, A., Senta Loys, Z., Jones, D., Andrews, G., & Healy, A. M. (2019). Metformin Hydrochloride and Sitagliptin Phosphate Fixed Dose Combination Product Prepared Using Melt Granulation Continuous Processing Technology. *AAPS PharmSciTech*, *21*(1). https://doi.org/10.1208/s12249-019-1553-2

Published in:
AAPS PharmSciTech

Document Version:
Peer reviewed version

Queen's University Belfast - Research Portal:
Link to publication record in Queen's University Belfast Research Portal

Publisher rights
© American Association of Pharmaceutical Scientists 2019.This work is made available online in accordance with the publisher's policies. Please refer to any applicable terms of use of the publisher.

General rights
Copyright for the publications made accessible via the Queen's University Belfast Research Portal is retained by the author(s) and / or other copyright owners and it is a condition of accessing these publications that users recognise and abide by the legal requirements associated with these rights.

Take down policy
The Research Portal is Queen's institutional repository that provides access to Queen's research output. Every effort has been made to ensure that content in the Research Portal does not infringe any person's rights, or applicable UK laws. If you discover content in the Research Portal that you believe breaches copyright or violates any law, please contact openaccess@qub.ac.uk.

Download date:27. Aug. 2022

Metformin Hydrochloride and Sitagliptin Phosphate Fixed Dose Combination Product Prepared Using Melt Granulation Continuous Processing Technology

Jeremiah F. Kelleher[#1], Atif M. Madi[#1], Gareth C. Gilvary[2], Y. W. Tian[2], Shu. Li[2], Ammar Almajaan[2], Zoe S. Loys[2], David S. Jones[2], Gavin P. Andrews[2], Anne Marie Healy[1*]

Affiliation

[1]School of Pharmacy and Pharmaceutical Sciences, Trinity College Dublin, Dublin, Ireland.

[2]Pharmaceutical Engineering Group, School of Pharmacy, Queen's University Belfast, Belfast, Northern Ireland.

# Both authors contributed equally to this work

*Corresponding author:

Prof. Anne Marie Healy

Tel: +35318961444

Email: healyam@tcd.ie

Abstract

The development of oral solid dosage forms, such as tablets, that contain a high dose of drug(s) requires polymers and other additives to be incorporated at as low levels as possible, to keep the final tablet weight low, and correspondingly the dosage form size small enough to be acceptable from a patient perspective. Additionally, a multi-step batch-based manufacturing process is usually required for production of solid dosage forms. This study presents the development and production, by twin-screw melt granulation technology, of a high-dose immediate-release fixed dose combination product of metformin hydrochloride (MET) and sitagliptin phosphate (SIT), with drug loads of 80 % w/w and 6 % w/w, respectively. For an 850/63 mg dose of MET/SIT, the final weight of caplets was approximately 1063 mg compared with 1143 mg for the equivalent dose in Janumet®, the marketed product. Mixtures of the two drugs and polymers were melt granulated at temperatures below the individual melting temperatures of MET and SIT (231.65 °C and 213.89 °C, respectively), but above the glass transition temperature or melting temperature of the binder used. By careful selection of binders, and processing conditions, direct compressed immediate release caplets with desired product profiles were successfully produced. The melt granule formulations before compression showed good flow properties, were larger in particle size than individual starting API materials and were easily compressible. Melt granulation is a suitable platform for developing direct compressible high-dose immediate release solid dosage forms of fixed dose combination products.

Key words:

Fixed dose combinations, hot melt extrusion, melt granulation, continuous manufacturing, high dose compounds.

Introduction

Diabetes mellitus is a metabolic disorder associated with high blood glucose levels (hyperglycemia) as a result of defects in insulin secretion and/or insulin action (1). Glucose is vital in maintaining a person's health as it is the main energy source for cells that make up muscles and tissues. It is also the brain's main fuel source (2). However, excess amounts of glucose in the bloodstream can result in severe medical complications. There are two main chronic forms of diabetes, type 1 and type 2, which can generally be categorized by their respective pathogenesis, clinical presentation and treatment requirements. Type 2 diabetes mellitus accounts for about 90 % of all diabetes cases and is characterised by insulin resistance at target cells and a relative rather than absolute deficiency in insulin activity which is associated with type 1 diabetes mellitus (3). Metformin hydrochloride (MET) is a biguanide with antihyperglycemic effects, lowering both basal and postprandial plasma glucose. It is the most widely used oral antidiabetic agent in type 2 diabetes and has been marketed since 1957. The dose of MET may vary from 500 mg once daily up to 1000 mg three times daily depending on response. MET exerts its effect by reduction of hepatic glucose production by inhibiting gluconeogenesis and glycogenolysis, increasing insulin sensitivity in muscle and delaying intestinal glucose absorption (4). MET is classified according to the Biopharmaceutics Classification System (BCS) as a BCS class III drug, which means that it shows high solubility and poor permeability characteristics. When MET monotherapy is unsuccessful at achieving satisfactory blood glucose control, a second anti-diabetic agent is often added to a patient's medication regimen. Sitagliptin phosphate (SIT) is a dipeptidyl peptidase-4 (DPP-4) inhibitor and works to control blood glucose levels by preventing the degradation of glucagon like peptide-1 agonist (GLP-1). It is also classified as a BCS class III drug. GLP-1 is degraded by DPP-4 and is one of two incretin hormones that stimulate insulin release and inhibit glucagon secretion, suppressing gastric emptying, and reducing appetite and food intake (5). DPP-4 inhibitors preserve β-cell mass through stimulation of cell proliferation, stimulating insulin secretion and inhibiting glucagon secretion (5).

MET and SIT are currently available as a fixed dose combination (FDC) product on the market in the form of Janumet®, a tablet product manufactured by Merck. Janumet® is available as 850/50 mg and 1000/50 mg metformin hydrochloride/sitagliptin (as sitagliptin phosphate monohydrate) film-coated tablets. By definition, a FDC product is a combination product that includes two or more Active Pharmaceutical Ingredients (APIs) combined in a single dosage

form, which is manufactured and distributed in fixed doses (6). FDC products are seen as advantageous for people requiring several medications to treat a target disease as they reduce the pill burden (7–9), can have synergistic or additive effects on pharmacological actions and result in cost reduction for both the patient and the manufacturer.

Melt granulation (MG), which is also often referred to as thermoplastic granulation, is a technique that facilitates the agglomeration of powder particles, using excipients which melt or soften at relatively low temperature, to form granules (10). The most common production technique for MG uses extruders, but MG in high-shear mixers has also been extensively described in the literature. The mechanism of MG is essentially like that of wet granulation with the main difference being, unlike wet granulation, no solution or liquid, such as water, is added to the powder bed before or during processing (11). Instead, the active pharmaceutical ingredient (API) is subjected to temperatures below its melting temperature but above the glass transition temperature (T_g) or melting temperature of the solid excipients used as polymeric binders. Once the melting of the binders and mixing with the API(s) has occurred, the mixture is then subjected to lower temperatures where, in an extruder, the mixture solidifies and produces granules at the end of the extruder barrel. MG has the advantage over other types of granulators in being designed for continuous processing. Additionally, MG has been reported to be beneficial in enhancing compactability, densifying granules, enhancing flowability, reducing segregation, and decreasing the generation of dust of pharmaceutical materials (11,12). It also has the advantage of being seen as a "green technology", as no solvents are required, and it is easily scaled up (13).

The main aim of the current work was to investigate the viability of twin-screw melt granulation as a continuous processing technique to produce a monolithic high dose FDC product of MET and SIT. Additionally, the study aimed to investigate the effect of different binder grades and processing conditions on the characteristics of the produced granules as well as the in vitro performance of the subsequent compressed caplets.

Materials and Methods

Materials

Metformin hydrochloride (MET) was purchased from Tokyo Chemical Industry UK Ltd. (Oxford, UK) and sitagliptin phosphate (SIT) was purchased from Kemprotec (Carnforth, UK). Three hydroxypropyl cellulose (HPC) grades were studied as carrier polymers/meltable binders and their characteristics are detailed in Table I. HPC-A was obtained from Ashland (Covington, Kentucky, USA), HPC-S was received from Sigma-Aldrich (Dorset, UK) and L-HPC was obtained from Shin-Etsu (Wiesbaden, Germany). Polyethylene glycol (3350 g/ mol) was purchased from Sigma-Aldrich (Dorset, UK). Microcrystalline cellulose, Avicel PH102, was received from IMCD Ltd. (Sutton, UK). Deionised water was obtained using an Elix 3 connected to a Synergy® UV water purification system (Millipore, UK). All other chemicals were obtained from Sigma-Aldrich (Dorset, UK) and were of analytical grade or equivalent and were used without any further treatment.

Methods

Solid state characteristics

Thermogravimetric Analysis (TGA)

Thermogravimetric analysis studies were conducted using a TGA Q50 (TA Instruments, Leatherhead, UK) to evaluate the onset of degradation of each of the individual ingredients. Samples (5–10 mg) were analysed in open standard aluminium pans using a linear heating rate of 10 °C/min from 50 to 400 °C. TGA data was analysed using TA Universal Analysis software version 4.5A (TA Instruments, Leatherhead, UK). Analysis was performed in triplicate.

Differential Scanning Calorimetry (DSC)

The thermal behaviour of materials was analysed using a differential scanning calorimeter (Q200, TA Instruments, Leatherhead, UK). Nitrogen was used as the purge gas (60 ml/min). Temperature and cell constant calibration was performed with an indium standard. Samples (5–10 mg) were analysed in crimped standard aluminium pans with a heating rate of 10 °C/min. DSC data was analysed using TA Universal Analysis software version 4.5A (TA Instruments, Leatherhead, UK). Melting temperatures of drugs were determined and reported as peak temperature. The glass transition temperatures were defined as the midpoint of the transition.

HPC polymers were heated to 140 °C, held for 5 min to remove any moisture present, and cooled to – 40 °C before being heated at a heating rate of 10 °C/min to determine the glass transition and melting temperatures. Analysis was performed in triplicate.

Powder X-ray Diffraction (PXRD)

Powder x-ray diffraction studies were conducted to determine the solid-state nature of API raw materials, polymers, physical mixtures and manufactured melt granulate formulations. PXRD was performed on a Mini-Flex II (Rigaku™ Corporation, Japan) with Cu Kα radiation (30 kV) in the angular range (2θ) varying from 5 to 40° using a step scan mode with a step width of 0.05° and a counting time of 2 s/ step. Scans were performed in triplicate at room temperature.

Manufacture of Twin-screw Melt Granules

Formulations of HPC and APIs were physically mixed for 5 minutes, using a mortar and pestle. Mixed powders were manually fed into a co-rotating 20:1 (screw length to diameter ratio), fully intermeshing twin-screw Rondol Microlab 10 mm extruder (Rondol Technology Ltd., France) with only forward conveying elements assembled and no die attached (open end) (Table II). The ratio of MET to SIT was kept constant at 850:63, which corresponds to a dose ratio of 850 mg of MET and 50 mg of sitagliptin. This is comparable to the already commercialised FDC product containing MET and SIT. PEG 3350 was used, when necessary, as an additional binding agent to improve granule production and appearance, and was mixed with the other components using a mortar and pestle prior to granulation. The extruder barrel was divided into 4 heating zones (the feeding zone and heating zones 1-3). Processing temperatures were set at 130 °C and incrementally increased up from the feed to the collect end. Screw rotation speed was varied between 5-20 rpm during the development and optimisation stage of the study with 10 rpm being selected as the optimised screw rotation. Batch size remained constant at 5 grams per batch.

Characterisation of Melt Granules

Particle Size Analysis (PSA)

PSA was performed by laser diffraction using a Malvern Mastersizer 3000 particle sizer (Malvern Instruments Ltd, Worchester, UK) with Aero M dry powder dispersion accessory.

The dispersive air pressure used was 2 bar. Samples were run at a vibration feed rate of 50 %. The particle size reported is the median diameter d (50). The d (50) is the diameter where 50 % of the cumulative distribution is above and 50 % is below this size. The values presented are the average of at least three determinations. Mastersizer 3000 software (Version 3.50) was used for the analysis of the particle size.

Flowability Measurements

Flowability behaviour of physical powder blends and melt granules was determined using a FT4 powder rheometer (Freeman Technology, Tewkesbury, UK). Cohesiveness and angle of internal friction were determined by placing between 1 and 2 grams of samples in the 1 mL shear cell and applying a 24 mm shear head. The flowability for each sample following pre shearing at a pre-shear normal stress of 9 kPa was investigated by determining the angle of internal friction (AIF), cohesiveness and flow function (FF) (17). All samples were tested at least in triplicate and average values determined.

Content Assay Studies

50 mg of each manufactured formulation was accurately weighed using a microbalance (Mettler-Toledo, Leicester, UK), added to a 100 ml volumetric flask and made up to the mark with 0.1 M HCl solution. The solution was sonicated for 10 min to ensure the formulation was fully dissolved, filtered through 0.45 µm PTFE filters (Fisher Scientific Ireland Ltd., Dublin, Ireland), and diluted suitably to fall within the concentrations of the calibration curves for the individual APIs and then analysed by High Performance Liquid Chromatography (HPLC). The concentrations of MET and SIT in solution were determined using an Alliance HPLC with a Waters 2695 Separations module system and Waters 2996 photodiode array detector (Waters, Milford, MA, USA). The HPLC mobile phases consisted of a 0.01 M ammonium acetate solution adjusted to pH 4.5 with acetic acid (mobile phase A) and acetonitrile (mobile phase B). The ratio of mobile phase A to mobile phase B was 30:70 v/v. The mobile phase was vacuum filtered through a 0.45 µm membrane filter (Pall Supor® 0.45 µm, 47 mm) and bath sonicated for 5 min. Separation was achieved using a Zorbax CN (4.6 mm i.d., 250 mm and 5 µm) column, detection wavelength was 239 nm for MET and 267nm for SIT, flow rate of 1.0 ml/min and an injection volume of 10 µL. The elution times for MET and SIT were 11.1 min and 13.5 min respectively. Empower software was used for peak evaluation. Calibration curves were conducted weekly, with freshly prepared samples, while studies were on-going. The

linearity range was between 1 - 100 µg/ml for MET and 1 – 75 µg/ml for SIT with regression coefficient (r^2) of 0.999 and 0.998, respectively. The limits of detection for the method were 0.6 µg/ml for MET and 1.1 µg/ml for SIT. The HPLC method was validated for linearity, range, accuracy, precision and robustness as per ICH Q2 (R1) guidelines. Drug content was calculated by determining the area under the curve and comparing to area under the curve of standards of known concentration. Analysis was performed in triplicate.

Scanning Electron Microscopy (SEM)

SEM studies were conducted to visualise the morphology of raw materials and melt granule formulations. The surface images of the samples were captured at various magnifications by SEM using a Zeiss Supra Variable Pressure Field Emission Scanning Electron Microscope (Zeiss, Oberkochen, Germany) equipped with a secondary electron detector at 5kV. Samples to be studied, were glued onto carbon tabs mounted on to aluminium pin stubs and sputter-coated with a gold/palladium mixture under vacuum prior to analysis.

Caplet Manufacture

The manufactured and optimised melt granules with the highest possible drug loads were manually compressed into caplets using a Natoli single punch press (Natoli, USA). Additionally, the same formulations were blended with Avicel® PH102 (10 % (w/w)) using a Turbula mixer (Glen Creston Ltd., Basel, Switzerland) for 10 minutes at 60 rpm before being manually compressed into caplets using a Natoli single punch press (Natoli, USA). 1063 mg of each formulation (equivalent to 850 mg MET and 63 mg SIT) were weighed and compressed in an in house designed die (figure 1) using two different compression forces, 5000 N and 8000 N (I Holland Ltd, Nottingham, UK). When Avicel PH102 was added the total weight of each compressed caplet was 1170 mg. Conventional caplet quality control tests (weight variation, friability, hardness, disintegration, drug content, *in-vitro* dissolution) were conducted according to pharmacopoeia standards.

Caplet Characterisation

Hardness Test

A minimum of 6 individual caplets that were prepared at the different compression forces were subjected to a crushing test using an EH-01 Electrolab manual tablet hardness tester (Electrolab, Mumbai, India). Thickness (internal and external), diameter and length of caplets were first measured using a digital electronic external micrometer (RS PRO Micrometer External, 0 - 25 mm, Radionics Ltd., Dublin, Ireland) before placing at the moving jaw of the hardness tester. The long side of the caplet was oriented parallel to the direction of force. The force required to break the caplet was recorded in Newtons (N) and tensile strength was calculated according to equation 1 proposed by Pitt and Heasley below (18):

$$\sigma_t = \frac{2}{3}\left(\frac{10P}{\pi D^2\left(2.84\frac{t}{D} - 0.126\frac{t}{w} + 3.15\frac{w}{D} + 0.01\right)}\right) \quad \text{Equation 1}$$

Where:

σ_t= Tensile strength (MPa)

P= Fracture load (N),

D= diameter (mm)

t= thickness (external)

w= thickness (internal) (height)

L= length of long axis (mm)

Friability Studies

A sample of 10 caplets were carefully dedusted prior to testing, accurately weighed and placed in a Copley TA20 friability test drum (Copley Scientific, Nottingham, UK). The drum was rotated for 100 rpm at 25 rpm for 4 minutes as per the British Pharmacopoeia (BP) method (19). Caplets were dedusted and accurately weighed. Friability was calculated as per equation 2 below:

$$\% F = \frac{W_0 - W_1}{W_0} X\ 100 \qquad \text{Equation 2}$$

Where:

$\% F$ = percentage friability

W_0 = the initial total weight of caplets

W_1 = the total weight of caplets after the test.

Disintegration Studies

A minimum of 6 caplets were placed in the basket rack of a Erweka ZT 44 disintegration tester (Novatech, Newcastle, UK) which was immersed in a bath of 0.1 M HCl, pH 1.2, held at 37 °C with a constant vertical agitation rate of 30 cycles per minute as per the BP method (20). The volume of the fluid in the vessel was such that at the highest point of the upward stroke the wire mesh remained at least 15 mm below the surface of the fluid and descended to not less than 25 mm from the bottom of the vessel on the downward stroke. At no time was the top of the basket-rack assembly submerged. The time required for all the caplets to pass through the mesh screen was recorded.

In-vitro Dissolution Studies

In-vitro dissolution studies of the manufactured caplets were performed using a Sotax AT-7 USP type II paddle apparatus (Sotax, Wallbrunnstraße, Germany). The dissolution study was carried out using 0.1 M HCl as the dissolution medium (volume: 900 ml, temperature: 37 ± 0.5 °C, pH: 1.2) and a rotational speed of 50 rpm. This dissolution method was chosen to mimic the target release conditions of the stomach. 5 ml aliquots were withdrawn and were replaced with fresh media at the pre-determined time intervals. Samples were filtered through PTFE hydrophilic 0.45 µm filters (Fisher Scientific Ireland Ltd., Dublin, Ireland) and were analysed for drug content by HPLC as previously described. The dissolution study was terminated after 120 min. All studies were conducted in triplicate.

Statistical Analysis

Statistical analysis was conducted using Minitab® 16 software. A two-sample t-test was carried out to compare the effects of particle size for different melt granule formulations. A two-sample

t-test was carried out to compare the various flowability measurements of physical mixtures and melt granulation formulations. A one-way Analysis of Variance (ANOVA) was carried out to compare the various flowability measurements of physical mixtures, melt granulation formulations and melt granulation formulations with the addition of 10 % w/w glidant. A one-way ANOVA at each individual time point was used to compare the difference in drug release profiles of manufactured formulations. In all statistical analyses, $p < 0.05$ denoted significance.

Results and Discussion

Hydroxypropyl cellulosic (HPC) based polymers have been successfully employed in previous melt-granulation studies for high dose drugs, including MET (11,13,21), because of their high binding ability behaviour (22,23). Lakshman *et. al*. reported that MET was compatible with HPC polymers (22). As formulations with drug loads of up to 90 % have been successfully achieved using the MG process and reported in the literature, it was an aim of this study to minimise the amount of HPC required to manufacture successful granules comprising two APIs. Initial trials with HPC-A and HPC-S with drug loading of MET alone proved successful at granule formation with API loading up to 85 % w/w. Initial trials using L-HPC at various ratios with MET alone (trialling 30:70, 40:60, 50:50, 60:40 L-HPC: MET % w/w), various screw rotation speeds (5 – 20 rpm) and processing temperatures proved unsuccessful at granule formation. This is thought to be due to the poor binding properties of L-HPC polymer which makes it unsuitable for use in MG studies with MET. As shown in Table I, L-HPC has a very low level of substitution of hydroxypropyl groups on the cellulose backbone, which means that less binding groups are available, in order to achieve binding between the API and polymer, compared to the other HPC grades used. Previous studies also suggest that L-HPC is suitable for wet granulation applications or other aqueous based methods, but not MG (24,25). Subsequently, L-HPC was excluded from further work, with the focus being only on the other two grades of HPC (i.e. HPC-A and HPC-S).

Solid state characteristics of raw materials

As MG employs thermal energy during the process, it is important to know the thermal degradation points of each of the components to be added to the formulations for MG studies. Figure 2 shows the various thermal degradation temperatures by TGA for the different components used in developing the final formulations. MET has previously been reported to be thermally stable over a wide range of temperatures (26) and was found by TGA to be thermally stable up to 230.52 ± 1.62 °C (figure 2 (a)). SIT also showed thermal stability up to 216.21 ± 2.73 °C (figure 2 (b)), which was consistent with a previous report (27). It is worth noting that there was some weight loss in SIT samples between approximately 90 ºC and 126 °C, corresponding to 3.34 % w/w of the initial sample weight; this loss in weight can be attributed to the single water molecule within the initial starting monohydrate material. TGA studies of HPC samples indicated that their thermal degradation occurs at higher temperatures than the APIs. The HPC-S grade showed a thermal stability up to 294.16 ± 0.98 °C, whereas

HPC-A started to thermally decompose at 334.68 ± 1.89 °C. PEG 3350 started to thermally degrade at 355.45 ± 1.44 °C.

As HPC is a semi-crystalline polymer it has both amorphous and crystalline domains within the structure (28). The polymer itself is very hygroscopic, and as a result the T_g of the amorphous domain varies greatly with moisture content (29). Based on work conducted by Picker-Freyer and Dürig, crystallinity for the various grades of HPC is estimated to be between 7 % and 9 % (29). Figure 3 below, shows the second heating cycle of a heat-cool-heat cycle of both HPC-A and HPC-S to highlight the thermal characteristics of the polymers without any water content. The results correspond well to previous reports by Picker-Freyer and Dürig (2007). These authors reported the T_gs of the amorphous portion of HPC polymers to be close to 0 °C, while in the current study they were determined to be at 7.27 ± 0.35 and 9.66 ± 0.20 ºC for HPC-A and HPC-S respectively. HPC crystalline domains have been reported to display melting endotherms in the range of 180 °C to 220 °C (29), and the higher the molecular weight of the HPC polymer, the higher the melting endotherm. This is evident in figure 3, where HPC-A is shown to have a higher melting point, at 205.99 ± 1.31 °C, compared to HPC-S, at 194.73 ± 1.89 °C (29).

Standard DSC runs showed the starting API materials were crystalline in nature with sharp melting endotherms at 232.53 ± 1.20 °C and 213.48 ± 0.75 °C for MET and SIT, respectively (figure 4). With regards to the endotherm seen with SIT at 137.66 ± 1.15 °C, this can be attributed to the loss of a water molecule, as previously observed by TGA. PEG 3350 is a semi-crystalline plasticizer that exhibits a melting endotherm at 59.79 ± 0.04 °C (figure 4 (a)). As both MET and SIT start to thermally degrade near their melting temperatures, the MG process temperatures have to be set below the thermal degradation points of the APIs.

PXRD data (figure 5) supported the data obtained from DSC analysis, that the starting API materials were in the crystalline state. MET showed characteristic Bragg peaks at 12.25 °(2θ), 17.65 °(2θ), 22.40 °(2θ) and 39.50 °(2θ), which are consistent with the literature (30,31). SIT showed characteristic Bragg peaks at 13.90 °(2θ), 16.10 °(2θ), 18.65 °(2θ), and 21.25 °(2θ),

which are also consistent with the literature (32). PEG 3350 showed characteristic Bragg peaks at 19.20 °(2θ) and 23.30 °(2θ), consistent with previous reports in the literature (33,34). The PXRD diffractograms for HPC-A and HPC-S are very similar, displaying "halo" patterns, which are characteristic of amorphous materials, centred at 8.55 °(2θ) and 20.35 °(2θ) respectively. While cellulose polymers consist of both crystalline and amorphous domains, the crystalline domain content is presumably so small, the amorphous halo dominates the PXRD pattern.

Manufacture of Melt granules

The initial visual characterisation of melt granules is essential when processing materials using a twin-screw melt granulation technique (12,35). Optimised melt granule formulations are expected to be solid, uniform in particle size distribution, show acceptable flow properties and have no charred spots (36,37). During the course of this study, during method development and optimisation, a range of processing parameters (screw rotation speed and processing temperatures), HPC grade and proportions were investigated to optimise the final melt granule formulation so that it exhibited acceptable visual characteristics upon manufacture.

The extruder barrel was divided into 4 heating zones (including the feeding zone and heating zones 1-3). The final temperatures chosen are displayed in table III. The temperature throughout remains below the melting temperatures of both APIs but above both HPC-A and HPC-S T_gs and above the melting temperature of PEG 3350. This allows for granules to form successfully. The temperature increases from the feed zone through to zone 3 to allow the complete melting/softening of the excipients while also allowing adequate time for the components to mix with one another during the process.

A disadvantage associated with working with FDC products is that the ratio of drugs needs to remain constant, in this case, for every 850 mg of MET we need 63 mg of SIT (equivalent to 50 mg of sitagliptin). For this reason, the only variation in formulation can come from the excipients added. Ideally, the final formulation should contain as little excipients as possible due to the already large API content required. HPC-S and HPC-A were successfully employed to produce granules which, from initial visual inspection, were larger in size compared to the physical mixtures fed into the extruder. Initial studies consisted of MET and HPC only as these components made up most of the formulation. It was possible to process MET drug loadings

as high as 85 % w/w using either of the two grades of HPC. However, the manufactured granules were slightly fragile and tended to break apart after they were cooled. While other studies have shown that MET may be successfully melt granulated up to 90 % w/w with HPC and other polymers using larger melt extruders (21,22), it is likely that this is because of the ability of larger extruders to exert relatively higher pressures and torque required for granule formation in comparison to the 10 mm lab-scale extruder used in this study. To overcome this problem, PEG 3350 was added to the formulation, as it was hypothesised that the melting of this low melting point hydrophilic substance would allow for better granule formation. PEGs are well suited to work as binders in granulation and have been successfully used for many years in various granulation techniques (38,39). Low molecular weight PEGs have been shown to produce more spherical particles than high molecular weight PEGs owing to differences in viscosity exerted during the MG process (38). The addition of the PEG at low concentration had the desired effects visually, with granules appearing more free flowing and less fragile.

Control studies using PEG 3350 alone were also conducted using the same process conditions and PEG concentrations of 5 %, 10 % and 15 % w/w with MET. At 5 % w/w PEG there was no noticeable difference between the initial physical mix and the product produced post MG. At 10 % and 15 % w/w, granules were not formed; rather large agglomerated masses of material resulted, and thus PEG 3350 alone was deemed unsuitable as a binder.

Finally, the second API, SIT, was added to the formulation and the final % w/w of each component is displayed in table III below. The optimised screw rotation speed was 10 rpm.

Characterisation of the Melt Granules

Differential Scanning Calorimetry (DSC)

Strong intermolecular interactions exist between MET and SIT which is evident by the decrease in melting temperatures seen in the physical mixture between the two APIs (figure 6 (a)) in the FDC product ratio, 850:63. SIT melting point is significantly lowered to 188 °C, while MET melting point is also decreased to 227 °C. Figures 6 (b) and 6 (c) show DSC results for physical mixtures (PM) for constituents of both formulations chosen as the optimized formulations. Melting points are evident in both PMs for PEG, SIT and MET indicating crystallinity may be measured via DSC for the proportion used in the formulations. The lack of endothermic peaks

for PEG 3350 and SIT in the MG formulations (figure 6 (d) and 6 (e)), indicate that post processing, both components are present in a non-crystalline state, most likely in their amorphous states. MET remains fully crystalline. For MG formulations, the absence of a melting endotherm for SIT, which is evident in the PMs, can be explained by the API melting during the process. As the melting point is evident in the thermograms of the PMs, if SIT remained crystalline after MG then the same endotherms would be expected to be seen post processing. The DSC thermograms of the PMs also indicate that the quantity of SIT in the formulation is not soluble in the other excipients, which display melting points or T_gs lower than 186 °C, since, if SIT was soluble in these excipients, one would expect that no endotherm at 186 °C would be seen. Even though the highest temperature on the extruder during processing was 180 °C, local hot spots can form causing increases in temperature above the set point on the thermostats (40). It is most likely these hot spots allowed SIT to melt forming an amorphous form during the processing. MET remains fully crystalline in both MG formulations with no statistical difference between the heat of fusion for any of the PM and MG samples ($p > 0.05$).

Powder X-ray Diffraction (PXRD)

The PXRD patterns for PM and MG formulations are shown in figure 7. Bragg peaks displayed in the diffractograms of PMs (figure 7 (a) and (b)) are peaks associated with crystalline MET. Due to the high MET content in the formulations and the strong Bragg peaks associated with it, unique Bragg peaks associated with SIT and PEG 3350 are not detectable in the PMs. Thus, as a method of determining the solid state of SIT and PEG 3350 post processing, PXRD is unsuitable. However, it remains a suitable technique to determine the solid state of MET. For MG formulations, MET remains in the crystalline state post processing as is evident with characteristic Bragg peaks remaining. Two MET polymorphs have previously been reported in the literature, the stable form A and a metastable form B (41,42). The MET raw material used during the study was form A. The positions of the strong diffraction peaks are the same for all PM and MG formulations, indicating the same crystal lattice and implying no MET polymorph form change in MET during processing. While we see a difference in peak intensity of the different formulations, this may be explained by the preferential orientation of the crystals within the sample holder (43).

Particle Size Analysis (PSA)

Particle size plays an important role in many aspects of the manufacturing process. In general, smaller particles demonstrate stronger interparticular cohesive forces compared to larger particles, which in turn affects the flowability. Typically, granulation aims to increase particle size of formulations to form granules (usually between 200 μm and 4000 μm) by creating bonds between particles by compression or by using binding agents. Particle size analysis (PSA) results are presented in table IV for the APIs and MG formulations. As MET comprised the majority of the formulations (80 %), the particle size of the MET raw material was compared to the MG formulations particle size. The median particle size of MG formulations were statistically larger than the MET raw material ($p < 0.05$). As the MG process resulted in particles larger than the MET raw material, and were larger than 200 μm, the process conditions were considered to have resulted in successful granule manufacture for both HPC grades.

Flowability measurements

Flowability measurements are essential, as poorly flowing particles or powder blends are problematic in the manufacturing of solid dosage forms, such as compressed tablets or powder-filled hard gelatin capsules (44). Powder flow characteristics are determined by both the physical properties of the powders such as particle size, distribution and shape and are also determined by several environmental factors such as temperature, humidity and the stresses applied during storage and processing, such as gravity, vibrations, air pressure, and external loading from filling devices (45). As the products being tested varied in particle size, the initial state of the products before testing is particularly important and so “conditioning” to ensure a reproducible packing condition is essential if the data is to be reproducible, repeatable and comparable (17). Once consolidation has been completed and shear testing has been performed, several different results may be determined, including the measured Angle of Internal Friction (AIF) and cohesion, which can be directly used to assess the product’s flowability. The AIF is defined as a measure of the ability of a unit of product to withstand a shear stress. It is the angle (φ), measured between the normal force and resultant force that is attained when failure just occurs in response to a shearing stress. The AIF values have been shown to be directly related to particle size and shape (17,46). Previously, it was reported that the AIF plays a significant role in determining the flow function (FF) of powders and granules (17,46,47). Recently

however, Wang *et al.* (48) reported that, while, by definition FF requires the AIF be known, in practice the AIF plays a very limited role, and cohesive factors are much more critical in determining powder flowability. Correlation between FF and cohesion can be sustained as long as the AIF at incipient flow is not significantly larger than the AIF at steady-state flow, a condition covering almost all pharmaceutical powders. These findings were confirmed by Leung *et al.* (49) when the experimental conditions were undertaken using a much larger sample size.

Results of AIF, cohesiveness and FF are shown in table V for PMs of HPC-A and HPC-S formulations, MGs of HPC-A and HPC-S formulations and MGs of HPC-A and HPC-S formulations with the addition of 10% w/w glidant. For HPC-S formulations, statistically there was no difference between the PM and MG formulations in their respective AIF, cohesiveness and FF results ($p > 0.05$). For HPC-A formulations, the same observation was made with no difference between the PM and MG formulations in their respective AIF, cohesiveness and FF results ($p > 0.05$). Avicel PH102 is a brand of microcrystalline cellulose (MCC) that has been used in processing to improve flowability while also reporting to improve compaction of powers due to its plastic properties (50,51). To try and improve the flowability parameters of the MGs formulations relative to the PMs, 10 % w/w Avicel was added to each formulation. While the concentration of Avicel PH102 added to formulations varies greatly throughout the literature, one of the goals of the current study was to ensure the minimum quantity of excipients as possible was used, hence 10 % w/w was chosen in order to keep the final formulation suitable for patient consumption. However, no significant changes in AIF, cohesiveness or FF were seen upon addition of the glidant for either formulation ($p > 0.05$). The average particle size for Avicel PH102 is 100 µm according to the manufacturer's specifications. Due to the relatively low concentration of Avicel PH102 and the smaller particle size compared to the MG formulations, it exerts no significant effects on flowability measurements. Also, Avicel PH102 at 10 % w/w concentration was compressed into caplets but did not significantly affect the caplet hardness, friability, disintegration or *in-vitro* dissolution studies of either formulation and these results were excluded from the current work.

Several other factors can have significant effects on the flowability of products such as moisture content, storage conditions and hopper angle. Jenike (52) used FF to classify powder

flowability, with higher values representing easier flow, as shown in table VI. All formulations tested are considered to be easy flowing based on the classification.

Content Assay

During processing, degradation of APIs may occur and as a result it is important to investigate the final API content to comply with regulations. During MG, thermal degradation is a potential hazard for APIs due to excess thermal energy generation. Acceptable limits of API content are usually stipulated in the monographs of pharmacopoeias. In the BP, no monograph currently exits for FDCs containing both MET and SIT. For individual monographs of MET and SIT, the requirement for content assay tests to be successful is to have drug content not less than 95.0 % and not more than 105.0 % of the stated amount (53,54). Table VII shows content assay for MET and SIT for all MG processed formulations, with all results complying with the required content of APIs.

Scanning Electron Microscopy

SEM images for API raw materials (MET and SIT) show both APIs to consist of orthorhombic-shaped crystals (figure 8 (a) and (b)). Figures 8 (c) and 8 (d) show SEM images for the MG formulations containing HPC-A and HPC-S respectively. The formulations appear as round agglomerates of smaller particles, with the loss of the longitudinal orthorhombic structures of the individual API raw materials. This corresponds well to the increase in the particle size, discussed above, of the MG formulations in comparison to the APIs raw materials.

Manufacture of Caplets

Due to the large therapeutic dosage of the APIs, conventional circular tablets with flat faces are unsuitable for patients to swallow easily. As the market product Janumet®, is manufactured to produce an elongated tablet, otherwise known as a caplet, it was decided that our in-house caplet die would be used to produce a similarly shaped product for ease of swallowing (figure 9). Two different compression forces were selected for caplet formation and the manufactured caplets were subjected to evaluation according to the common compendial tests for oral tablets (i.e. hardness, friability, disintegration and *in-vitro* dissolution).

Characterisation of Caplets

Caplet hardness testing

The strength of manufactured caplets can be defined in terms of the compression force required to fracture a specimen across its diameter, which is commonly determined by conducting a hardness test (55). The hardness of complex dosage forms, such as elongated caplets, may be determined using a crushing method, however, the breaking load does not take into consideration all dimensions and shape of such complex geometries. Thus, converting fracture loads to tensile strength, allows the determination of resistance to crushing while also taking into consideration the geometry of the tablets being tested (18). Table VIII shows the measured dimensions of the MG caplets manufactured post different compression forces. The length of the short axis (D) and the length of the long axis (L) show no statistical differences ($p > 0.05$) regardless of formulation or compression force used. However, for overall thickness (t) and tablet wall height (w), increased compression force resulted in significantly smaller caplets, as expected. HPC has previously been described as being a visco-elastic material (29), meaning increased compression forces result in greater compaction. The results here also correspond well with Picker-Freyer and Dürig's (29) findings that compactability is significantly affected by the molecular weight of HPC polymers. These authors concluded that the lower the molecular weight of the HPC polymer, the higher the plasticity and compactibility. Our results show similar findings, with MG formulations containing HPC-S being more compact than the equivalent MG formulations containing HPC-A.

Due to the higher compactability and plasticity of the HPC-S formulations, HPC-S caplets are harder than the equivalent caplets produced with HPC-A (table IX). Figure 9(b) shows an example of the axial fracture that occurs when caplets exceed their fracture load.

Friability Studies

Friability is the tendency of a solid dosage from (e.g. caplet) to crumble, chip or break following compression, which could be caused by many factors such as: caplet design, insufficient excipients (e.g. binder) and low compression force during pressing. Caplets should be hard enough to withstand packaging and transport conditions, but also need to disintegrate in a reasonable time to allow for drug dissolution to occur (56,57). The BP sets the standard

for friability testing, with a maximum loss of mass (obtained from a single test or from the mean of 3 tests) not greater than 1.0 % considered acceptable for most products (19). Friability results for MG caplets are shown in table X. For MG caplets, MG HPC-S, compressed at 8000 N, is the only MG caplet formulation to pass friability.

Disintegration Studies

Disintegration refers to the mechanical break up of a compressed tablet into small granules upon ingestion and therefore it is characterised by the breakdown of the interparticulate bonds, which were forged during the compaction of the tablet (58). Oral solid dosage forms are required to break apart or disintegrate in a reasonable period of time when brought into contact with a liquid medium to allow for the APIs contained in the dosage forms to be released (59,60). In addition to the solubility of components of the solid dosage form and the type of disintegration medium, it is well documented that the more compact the solid dosage form the more the time it needs to disintegrate, and hence very compressed caplets may show longer disintegration times (59,61). Table XI shows disintegration times for each of the manufactured caplets compacted at different compression forces. For uncoated oral tablets with an immediate release profile, the BP states that, tablets must be fully disintegrated within 15 min in order to comply with standards (62). All MG caplets passed the disintegration test, with caplets fully disintegrated within 15 min. MG HPC-A formulation caplets disintegrated statistically quicker ($p < 0.05$) than the equivalent MG HPC-S formulation caplets due to differences in tablet hardness, tablet size and porosity. Each of these factors has previously been described as having an influence on the disintegration times of oral solid dosage forms (58).

In-Vitro Dissolution Studies

In-vitro drug dissolution studies were undertaken for the MG HPC-A and HPC-S caplets, and results compared to dissolution profiles obtained for Janumet® (figure 10) as a reference. Dissolution conditions were chosen to mimic conditions in the stomach, the target release region for the caplets. All MG caplets fully released both MET and SIT within 10 min and 5 min respectively (figure 10). Interestingly, the compression force applied to manufactured caplets had no influence on rate of release of both drugs. As both MET and SIT are BCS class

III drug compounds, absorption is permeation rate limited and bioavailability is independent of drug release from the dosage form. From a regulatory point of view, BCS class III drug compounds can qualify for BCS based biowaivers which in turn lead to a reduction in initial set up costs for getting a product to market. To qualify for a BCS class III biowaiver, the test product must have very rapid dissolution profiles (> 85 % in the first 15 min) and the test product formulation is qualitatively the same and quantitatively very similar to the reference product (63). This is due to BCS Class III drug substances being more susceptible to the effects of excipients and because they may have site-specific absorption, there are a large number of mechanisms through which excipients can affect their absorption (64).

Conclusion

The continuous manufacturing of fixed dose combination products is beneficial in pharmaceutical manufacturing, where there has been increased interest in recent years in moving away from batch-based processes due to their limitations. The melt granulation technique employed in this study shows the potential application of the process for its implementation in a continuous manufacturing environment for large fixed dose combination formulations. Manufactured caplets had a smaller mass than the marketed equivalent. Caplets that passed all compendial tests for solid oral dose immediate release products can be successfully manufactured using melt granulation. However, many factors including machine parameters, polymer composition and compression forces used for final caplet compaction all impact the final product characteristics. Additionally, as metformin is indicated for treatment in type II diabetes in combination with several other active pharmaceutical ingredients, further work could be done to assess the suitability of melt granulation to produce fixed dose combination products of metformin and other active pharmaceutical ingredients.

Acknowledgements

This investigation was conducted with the financial support of both the Department for the Economy of Northern Ireland and Science Foundation of Ireland (SFI) under Grant Number 14/IA/2559.

AM Healy also acknowledges funding from Science Foundation Ireland (SFI) [Grant Number 12/RC/2275], co-funded under the European Regional Development Fund.

References

1. American Diabetes Association AD. Diagnosis and classification of diabetes mellitus. Diabetes Care [Internet]. 2011 Jan 1 [cited 2018 Mar 15];34 Suppl 1(Supplement 1):S62-9. Available from: http://www.ncbi.nlm.nih.gov/pubmed/21193628

2. Mayo Clinic. Diabetes - Symptoms and causes - Mayo Clinic [Internet]. 2018 [cited 2018 Mar 21]. Available from: https://www.mayoclinic.org/diseases-conditions/diabetes/symptoms-causes/syc-20371444

3. Zimmet P, Alberti KGMM, Shaw J. Global and societal implications of the diabetes epidemic. Nature [Internet]. 2001 [cited 2018 Mar 22];414:782–7. Available from: https://www.nature.com/articles/414782a.pdf

4. Merck. Glucophage Film-Coated Tablets - Summary of Product Characteristics (SPC) [Internet]. 2016 [cited 2018 Mar 26]. Available from: http://www.medicines.ie/medicine/3578/SPC/Glucophage+Film-Coated+Tablets/#PHARMACODYNAMIC_PROPS

5. Drucker DJ, Nauck MA. The incretin system: glucagon-like peptide-1 receptor agonists and dipeptidyl peptidase-4 inhibitors in type 2 diabetes. Lancet [Internet]. 2006 Nov 11 [cited 2018 Mar 26];368(9548):1696–705. Available from: https://www.sciencedirect.com/science/article/pii/S0140673606697055

6. Gautam CS, Saha L. Fixed dose drug combinations (FDCs): Rational or irrational: A view point. Br J Clin Pharmacol. 2008;65(5):795–6.

7. Cheong C, Barner JC, Lawson KA, Johnsrud MT. Patient adherence and reimbursement amount for antidiabetic fixed-dose combination products compared with dual therapy among texas medicaid recipients. Clin Ther [Internet]. 2008 Oct 1 [cited 2019 Jan 17];30(10):1893–907. Available from: https://www.sciencedirect.com/science/article/pii/S014929180800324X

8. Pan F, Chernew ME, Fendrick AM. Impact of Fixed-Dose Combination Drugs on Adherence to Prescription Medications. J Gen Intern Med [Internet]. 2008 [cited 2019 Jan 17];23(5):611–4. Available from: https://link.springer.com/article/10.1007/s11606-008-0544-x

9. Gerbino PP, Shoheiber O. Adherence patterns among patients treated with fixed-dose combination versus separate antihypertensive agents. Am J Health Syst Pharm [Internet]. 2007 Jun 15 [cited 2019 Jan 17];64(12):1279–83. Available from: http://www.ncbi.nlm.nih.gov/pubmed/17563050

10. Shanmugam S. Granulation techniques and technologies: recent progresses. Bioimpacts [Internet]. 2015 [cited 2019 Mar 25];5(1):55–63. Available from: http://www.ncbi.nlm.nih.gov/pubmed/25901297

11. Vasanthavada M, Wang Y, Haefele T, Lakshman JP, Mone M, Tong W, et al. Application of Melt Granulation Technology Using Twin-screw Extruder in Development of High-dose Modified-Release Tablet Formulation. J Pharm Sci [Internet]. 2011 May 1 [cited 2019 Mar 25];100(5):1923–34. Available from: https://www.sciencedirect.com/science/article/pii/S0022354915321626

12. Repka M a, Battu SK, Upadhye SB, Thumma S, Crowley MM, Zhang F, et al. Pharmaceutical applications of hot-melt extrusion: Part II. Drug Dev Ind Pharm. 2007;33(10):1043–57.

13. Vaingankar P, Amin P. Continuous melt granulation to develop high drug loaded sustained release tablet of Metformin HCl. Asian J Pharm Sci [Internet]. 2017 Jan 1 [cited 2019 Mar 25];12(1):37–50. Available from: https://www.sciencedirect.com/science/article/pii/S1818087616300769

14. Ashland. Klucel hydroxypropylcellulose, physical and chemical properties. [Internet]. 2017 [cited 2019 May 20]. Available from: https://www.ashland.com/file_source/Ashland/Product/Documents/Pharmaceutical/PC_11229_Klucel_HPC.pdf

15. Sigma Aldrich. Hydroxypropyl cellulose [Internet]. 2019. Available from: https://www.sigmaaldrich.com/catalog/product/aldrich/191884?lang=en&region=IE

16. Shin-Etsu. L-HPC [Internet]. 2019 [cited 2019 May 20]. Available from: https://www.shinetsupharmausa.com/en/pharma_excipients/l_hpc/index.pmode

17. Freeman R. Measuring the flow properties of consolidated, conditioned and aerated powders — A comparative study using a powder rheometer and a rotational shear cell. Powder

721 Technol [Internet]. 2007 May 16 [cited 2019 Apr 8];174(1–2):25–33. Available from:
722 https://www.sciencedirect.com/science/article/pii/S0032591006004475

723 18. Pitt KG, Heasley MG. Determination of the tensile strength of elongated tablets.
724 Powder Technol [Internet]. 2013 Apr 1 [cited 2019 Apr 16];238:169–75. Available from:
725 https://www.sciencedirect.com/science/article/pii/S0032591011007467

726 19. British Pharmacopoeia. Appendix XVII G. Friability - British Pharmacopoeia
727 [Internet]. 2019 [cited 2019 Apr 17]. Available from: https://www.pharmacopoeia.com/bp-
728 2019/appendices/appendix-17/appendix-xvii-g--friability.html?date=2019-04-
729 01&text=friability

730 20. British Pharmacopoeia. Appendix XII A. Disintegration - British Pharmacopoeia
731 [Internet]. 2019 [cited 2019 Apr 17]. Available from: https://www.pharmacopoeia.com/bp-
732 2019/appendices/appendix-12/appendix-xii-a--disintegration.html?date=2019-04-01#f20901

733 21. Batra A, Desai D, Serajuddin ATM. Investigating the Use of Polymeric Binders in Twin
734 Screw Melt Granulation Process for Improving Compactibility of Drugs. J Pharm Sci
735 [Internet]. 2017 Jan 1 [cited 2019 May 2];106(1):140–50. Available from:
736 https://www.sciencedirect.com/science/article/pii/S0022354916416011

737 22. Lakshman JP, Kowalski J, Vasanthavada M, Tong W-Q, Joshi YM, Serajuddin ATM.
738 Application of Melt Granulation Technology to Enhance Tabletting Properties of Poorly
739 Compactible High-Dose Drugs. J Pharm Sci [Internet]. 2011 Apr 1 [cited 2019 Mar
740 25];100(4):1553–65. Available from:
741 https://linkinghub.elsevier.com/retrieve/pii/S0022354915322024

742 23. Arndt OR, Kleinebudde P. Influence of binder properties on dry granules and tablets.
743 Powder Technol [Internet]. 2018 Sep 1 [cited 2019 Mar 28];337:68–77. Available from:
744 https://www.sciencedirect.com/science/article/pii/S0032591017303522

745 24. McConville JT, Ross AC, Chambers AR, Smith G, Florence AJ, Stevens HN. The effect
746 of wet granulation on the erosion behaviour of an HPMC–lactose tablet, used as a rate-
747 controlling component in a pulsatile drug delivery capsule formulation. Eur J Pharm Biopharm
748 [Internet]. 2004 May [cited 2019 May 2];57(3):541–9. Available from:
749 http://www.ncbi.nlm.nih.gov/pubmed/15093604

25. Airaksinen S, Karjalainen M, Kivikero N, Westermarck S, Shevchenko A, Rantanen J, et al. Excipient selection can significantly affect solid-state phase transformation in formulation during wet granulation. AAPS PharmSciTech [Internet]. 2005 Jun 6 [cited 2019 May 2];6(2):E311–22. Available from: http://www.ncbi.nlm.nih.gov/pubmed/16353990

26. Sarkar D, Nandi G, Changder A, Hudati P, Sarkar S, Ghosh LK. Sustained release gastroretentive tablet of metformin hydrochloride based on poly (acrylic acid)-grafted-gellan. Int J Biol Macromol [Internet]. 2017 Mar [cited 2019 Mar 28];96:137–48. Available from: http://www.ncbi.nlm.nih.gov/pubmed/27956100

27. Priyadarshini R, Nandi G, Changder A, Chowdhury S, Chakraborty S, Ghosh LK. Gastroretentive extended release of metformin from methacrylamide-g-gellan and tamarind seed gum composite matrix. Carbohydr Polym [Internet]. 2016 Feb 10 [cited 2019 Mar 28];137:100–10. Available from: http://www.ncbi.nlm.nih.gov/pubmed/26686110

28. Sarode A, Wang P, Cote C, Worthen DR. Low-Viscosity Hydroxypropylcellulose (HPC) Grades SL and SSL: Versatile Pharmaceutical Polymers for Dissolution Enhancement, Controlled Release, and Pharmaceutical Processing. AAPS PharmSciTech [Internet]. 2013 Mar [cited 2019 Apr 18];14(1):151. Available from: http://www.ncbi.nlm.nih.gov/pubmed/23250708

29. Picker-Freyer KM, Dürig T. Physical mechanical and tablet formation properties of hydroxypropylcellulose: In pure form and in mixtures. AAPS PharmSciTech [Internet]. 2007 Oct 9 [cited 2019 Apr 1];8(4):82. Available from: http://www.ncbi.nlm.nih.gov/pubmed/18181552

30. Rebitski EP, Aranda P, Darder M, Carraro R, Ruiz-Hitzky E. Intercalation of metformin into montmorillonite. Dalt Trans [Internet]. 2018 Feb 27 [cited 2019 Apr 2];47(9):3185–92. Available from: http://xlink.rsc.org/?DOI=C7DT04197G

31. Ige PP, Gattani SG. Design and in vitro and in vivo characterization of mucoadhesive matrix pellets of metformin hydrochloride for oral controlled release: A technical note. Arch Pharm Res [Internet]. 2012 Mar 5 [cited 2019 Apr 2];35(3):487–98. Available from: http://www.ncbi.nlm.nih.gov/pubmed/22477196

778 32. Shantikumar S, Sreekanth G, SurendraNath K V., JaferValli S, Satheeshkumar N.
779 Compatibility study between sitagliptin and pharmaceutical excipients used in solid dosage
780 forms. J Therm Anal Calorim [Internet]. 2014 Mar 30 [cited 2019 Apr 2];115(3):2423–8.
781 Available from: http://link.springer.com/10.1007/s10973-013-3329-3

782 33. Baird JA, Olayo-Valles R, Rinaldi C, Taylor LS. Effect of Molecular Weight,
783 Temperature, and Additives on the Moisture Sorption Properties of Polyethylene Glycol. J
784 Pharm Sci [Internet]. 2010 Jan 1 [cited 2019 Apr 2];99(1):154–68. Available from:
785 https://www.sciencedirect.com/science/article/pii/S0022354916303719?via%3Dihub

786 34. Kelleher JF, Gilvary GC, Madi AM, Jones DS, Li S, Tian Y, et al. A comparative study
787 between hot-melt extrusion and spray-drying for the manufacture of anti-hypertension
788 compatible monolithic fixed-dose combination products. Int J Pharm [Internet]. 2018 Jul 10
789 [cited 2019 May 2];545(1–2):183–96. Available from:
790 https://www.sciencedirect.com/science/article/pii/S0378517318303016

791 35. Parikh DM. Handbook of pharmaceutical granulation technology [Internet]. Informa
792 Healthcare USA; 2010 [cited 2019 Apr 2]. 659 p. Available from:
793 https://www.crcpress.com/Handbook-of-Pharmaceutical-Granulation-
794 Technology/Parikh/p/book/9781439807897

795 36. Passerini N, Albertini B, González-Rodríguez ML, Cavallari C, Rodriguez L.
796 Preparation and characterisation of ibuprofen-poloxamer 188 granules obtained by melt
797 granulation. Eur J Pharm Sci [Internet]. 2002 Feb [cited 2019 Apr 2];15(1):71–8. Available
798 from: http://www.ncbi.nlm.nih.gov/pubmed/11803133

799 37. Shimpi S, Chauhan B, Mahadik KR, Paradkar A. Preparation and evaluation of
800 diltiazem hydrochloride-Gelucire 43/01 floating granules prepared by melt granulation. AAPS
801 PharmSciTech [Internet]. 2004 Jul 12 [cited 2019 Apr 2];5(3):e43. Available from:
802 http://www.ncbi.nlm.nih.gov/pubmed/15760076

803 38. Schæfer T, Mathiesen C. Melt pelletization in a high shear mixer. VIII. Effects of binder
804 viscosity. Int J Pharm [Internet]. 1996 Aug 9 [cited 2019 Apr 3];139(1–2):125–38. Available
805 from: https://www.sciencedirect.com/science/article/pii/0378517396045498

806 39. Van Melkebeke B, Vermeulen B, Vervaet C, Remon JP. Melt granulation using a twin-
807 screw extruder: A case study. Int J Pharm [Internet]. 2006 Dec 1 [cited 2019 Apr 3];326(1–
808 2):89–93. Available from:
809 https://www.sciencedirect.com/science/article/pii/S0378517306005576

810 40. Wagner JR, Mount EM, Giles HF, Wagner JR, Mount EM, Giles HF. Troubleshooting
811 Mechanical Extrusion Problems. Extrusion [Internet]. 2014 Jan 1 [cited 2019 May 20];315–
812 27. Available from:
813 https://www.sciencedirect.com/science/article/pii/B9781437734812000272

814 41. Childs SL, Chyall LJ, Bretnall AE, Clarke SG, Dunlap JT, Coates DA, et al. A
815 Metastable Polymorph of Metformin Hydrochloride: Isolation and Characterization Using
816 Capillary Crystallization and Thermal Microscopy Techniques. Cryst Growth Des [Internet].
817 2004 [cited 2019 Apr 17];4(3):441–9. Available from:
818 https://pubs.acs.org/doi/abs/10.1021/cg034243p

819 42. Bretnall AE, Clarke SG. Metformin Hydrochloride - Analytical profiles of drug
820 substances and excipients. Volume 25. Brittain HG, editor. Academic Press; 1998. 243-293 p.

821 43. Garekani HA, Ford JL, Rubinstein MH, Rajabi-Siahboomi AR. Formation and
822 compression characteristics of prismatic polyhedral and thin plate-like crystals of paracetamol.
823 Int J Pharm [Internet]. 1999 Sep 30 [cited 2019 Apr 17];187(1):77–89. Available from:
824 http://www.ncbi.nlm.nih.gov/pubmed/10502615

825 44. Lindberg N, Pålsson M, Pihl A, Freeman R, Freeman T, Zetzener H, et al. Flowability
826 Measurements of Pharmaceutical Powder Mixtures with Poor Flow Using Five Different
827 Techniques. Drug Dev Ind Pharm [Internet]. 2004 Jan 9 [cited 2019 Apr 8];30(7):785–91.
828 Available from: http://www.tandfonline.com/doi/full/10.1081/DDC-120040343

829 45. Freeman RE, Cooke JR, Schneider LCR. Measuring shear properties and normal
830 stresses generated within a rotational shear cell for consolidated and non-consolidated powders.
831 Powder Technol [Internet]. 2009 Mar 5 [cited 2019 Apr 8];190(1–2):65–9. Available from:
832 https://www.sciencedirect.com/science/article/pii/S0032591008002532

833 46. Guo Z, Chen X, Xu Y, Liu H. Effect of granular shape on angle of internal friction of
834 binary granular system. Fuel [Internet]. 2015 Jun 15 [cited 2019 Apr 8];150:298–304.
835 Available from: https://www.sciencedirect.com/science/article/pii/S0016236115001957

836 47. Podczeck F, Mia Y. The influence of particle size and shape on the angle of internal
837 friction and the flow factor of unlubricated and lubricated powders. Int J Pharm [Internet]. 1996
838 Nov 29 [cited 2019 Apr 11];144(2):187–94. Available from:
839 https://www.sciencedirect.com/science/article/pii/S0378517396047552

840 48. Wang Y, Koynov S, Glasser BJ, Muzzio FJ. A method to analyze shear cell data of
841 powders measured under different initial consolidation stresses. Powder Technol [Internet].
842 2016 Jun [cited 2019 Apr 8];294(294):105–12. Available from:
843 https://linkinghub.elsevier.com/retrieve/pii/S0032591016300687

844 49. Leung LY, Mao C, Srivastava I, Du P, Yang C-Y. Flow Function of Pharmaceutical
845 Powders Is Predominantly Governed by Cohesion, Not by Friction Coefficients. J Pharm Sci
846 [Internet]. 2017 Jul [cited 2019 Apr 8];106(7):1865–73. Available from:
847 https://linkinghub.elsevier.com/retrieve/pii/S0022354917302447

848 50. Signet. Avicel PH [Internet]. 2019 [cited 2019 May 20]. Available from:
849 http://www.signetchem.com/product.aspx?prdid=2

850 51. Thoorens G, Krier F, Leclercq B, Carlin B, Evrard B. Microcrystalline cellulose, a
851 direct compression binder in a quality by design environment—A review. Int J Pharm
852 [Internet]. 2014 Oct 1 [cited 2019 May 20];473(1–2):64–72. Available from:
853 https://www.sciencedirect.com/science/article/pii/S0378517314004840

854 52. Jenike AW. Storage and flow of solids. Bull 123, Eng Exp Station Univ Utah, USA.
855 1964;

856 53. British Pharmacopoeia. Metformin Tablets - British Pharmacopoeia [Internet]. 2019
857 [cited 2019 Apr 16]. Available from: https://www.pharmacopoeia.com/bp-2019/formulated-
858 specific/metformin-tablets.html?date=2019-01-01&text=Metformin

859 54. British Pharmacopoeia. Sitagliptin Tablets - British Pharmacopoeia [Internet]. 2019
860 [cited 2019 Apr 16]. Available from: https://www.pharmacopoeia.com/bp-2019/formulated-
861 specific/sitagliptin-tablets.html?date=2019-01-01&text=sitagliptin

862 55. Fell JT, Newton JM. Determination of Tablet Strength by the Diametral-Compression
863 Test. J Pharm Sci [Internet]. 1970 May 1 [cited 2019 Apr 17];59(5):688–91. Available from:
864 https://www.sciencedirect.com/science/article/pii/S0022354915373068

865 56. Seitz JA, Flessland GM. Evaluation of the Physical Properties of Compressed Tablets
866 I: Tablet Hardness and Friability. J Pharm Sci [Internet]. 1965 Sep 1 [cited 2019 Apr
867 17];54(9):1353–7. Available from:
868 https://www.sciencedirect.com/science/article/pii/S0022354915350899

869 57. Chowhan ZT. Moisture, Hardness, Disintegration and Dissolution Interrelationships in
870 Compressed Tablets Prepared by the Wet Granulation Process. Drug Dev Ind Pharm [Internet].
871 1979 Jan 20 [cited 2019 Apr 17];5(1):41–62. Available from:
872 http://www.tandfonline.com/doi/full/10.3109/03639047909055661

873 58. Markl D, Zeitler JA. A Review of Disintegration Mechanisms and Measurement
874 Techniques. Pharm Res [Internet]. 2017 [cited 2019 Apr 18];34(5):890–917. Available from:
875 http://www.ncbi.nlm.nih.gov/pubmed/28251425

876 59. Caramella C, Colombo P, Conte U, Ferrari F, Gazzaniga A, LaManna A, et al. A
877 physical analysis of the phenomenon of tablet disintegration. Int J Pharm [Internet]. 1988 Jun
878 1 [cited 2019 Apr 17];44(1–3):177–86. Available from:
879 https://www.sciencedirect.com/science/article/pii/0378517388901147

880 60. Quodbach J, Kleinebudde P. A critical review on tablet disintegration. Pharm Dev
881 Technol [Internet]. 2015 May 15 [cited 2019 Apr 17];1–12. Available from:
882 http://www.tandfonline.com/doi/full/10.3109/10837450.2015.1045618

883 61. Radwan A, Wagner M, Amidon G, Langguth P. Bio-predictive tablet disintegration:
884 effect of water diffusivity, fluid flow, food composition and test conditions. Eur J Pharm Sci
885 [Internet]. 2014 [cited 2019 Apr 17];57:273–9. Available from:
886 http://europepmc.org/abstract/med/24036239

887 62. British Pharmacopoeia. Tablets - British Pharmacopoeia [Internet]. 2019 [cited 2019
888 Apr 18]. Available from: https://www.pharmacopoeia.com/Publication/bp-2019/formulated-
889 general/tablets.html?date=2019-04-01&text=disintegration

890 63. European Medicines Agency. M9 Step 2b on biopharmaceutics classification system
891 based biowaivers [Internet]. 2019 [cited 2019 Jan 10]. Available from:
892 www.ema.europa.eu/contact

893 64. Wu C-Y, Benet LZ. Predicting Drug Disposition via Application of BCS:
894 Transport/Absorption/ Elimination Interplay and Development of a Biopharmaceutics Drug
895 Disposition Classification System. Pharm Res [Internet]. 2005 Jan 1 [cited 2019 Jan
896 11];22(1):11–23. Available from: http://link.springer.com/10.1007/s11095-004-9004-4

897

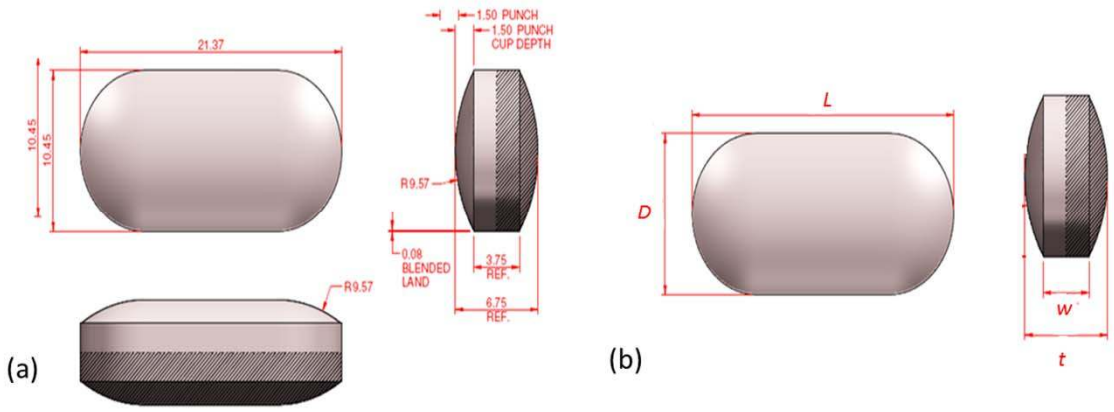

898

899 **Figure 1**. In-house design of manufactured caplets (a) and caplet shape and dimensions for
900 Equation 1 (b) *(18)*

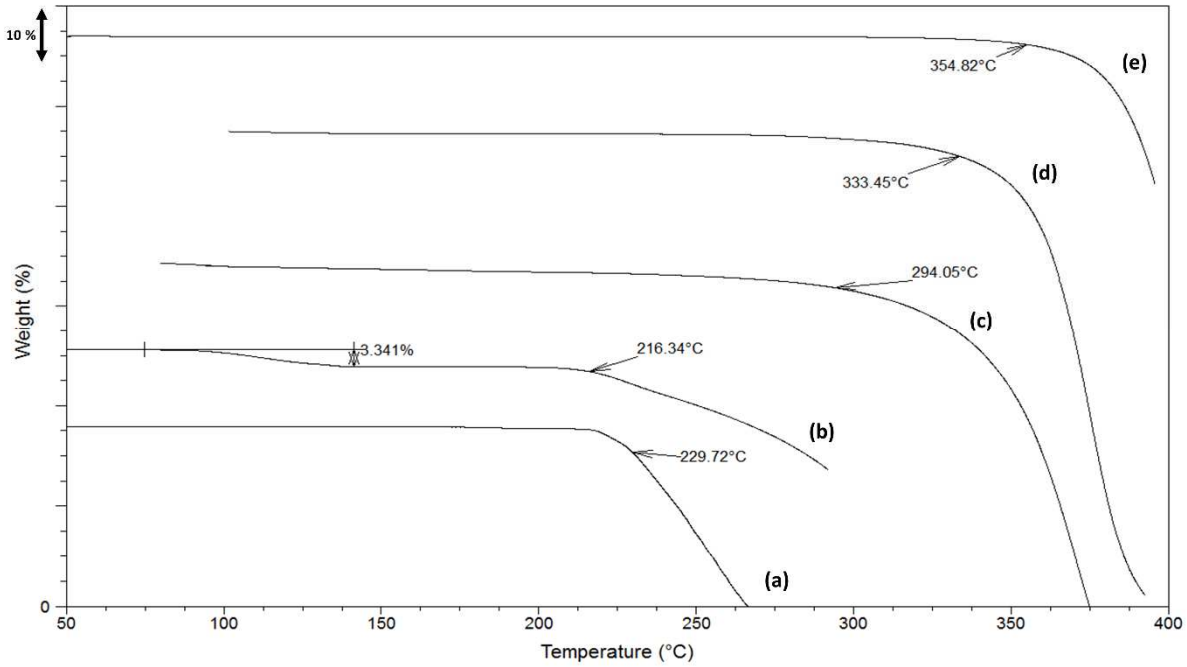

901

902 **Figure 2**. TGA thermograms of raw materials: (a) MET, (b) SIT, (c) HPC-S, (d) HPC-A and,
903 (e) PEG 3350.

904

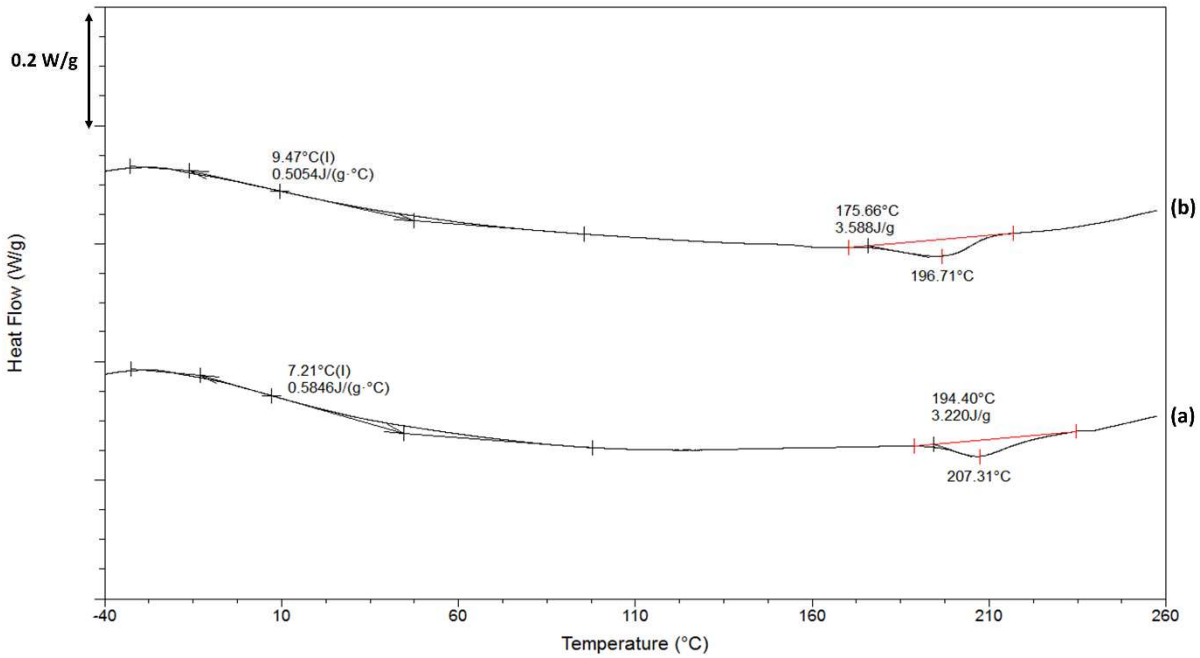

905

906 **Figure 3**: DSC thermogram of the second heating cycle in a heat-cool-heat cycle for (a) HPC-
907 A and (b) HPC-S.

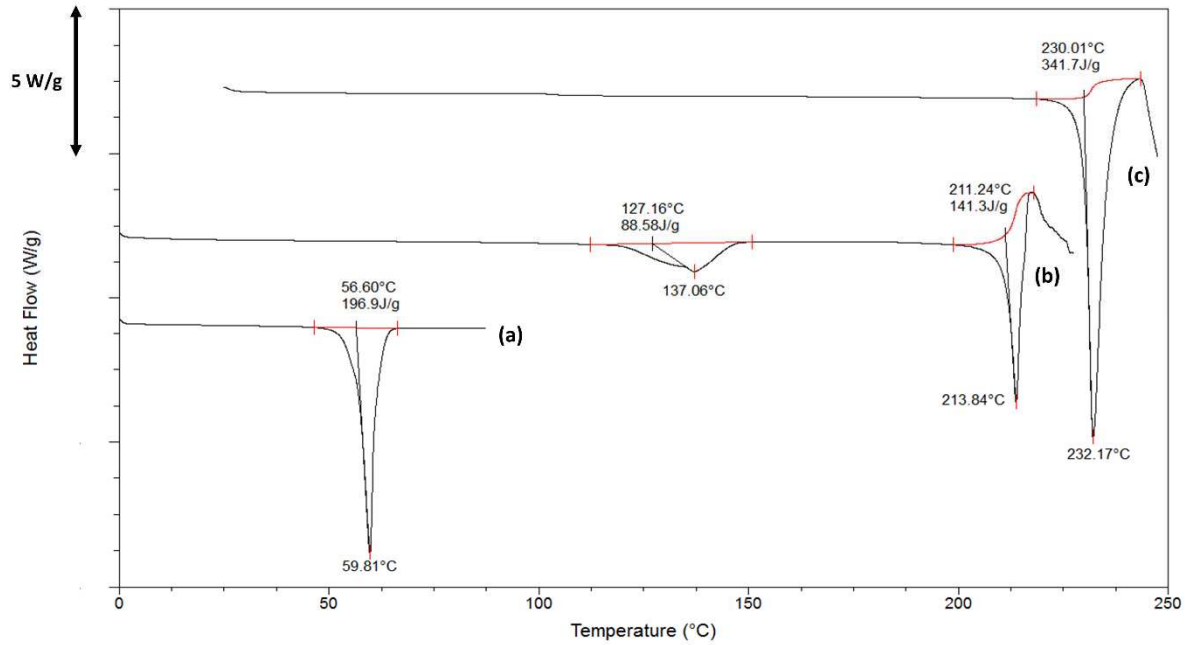

908

909 **Figure 4**. DSC thermogram of API raw materials: (a) PEG 3350, (b) SIT, (c) MET.

910

911

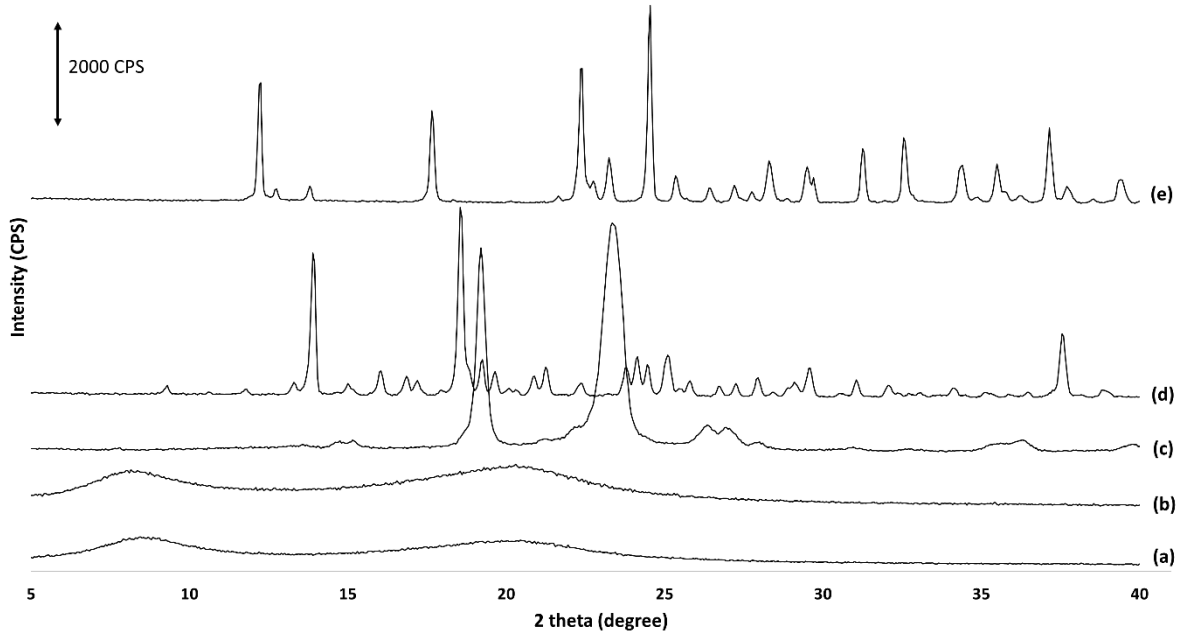

912

913 **Figure 5.** PXRD of raw materials over the range of 5–40° 2θ: (a) HPC-S, (b) HPC-A, (c) PEG
914 3350, (d) SIT, and (e) MET.

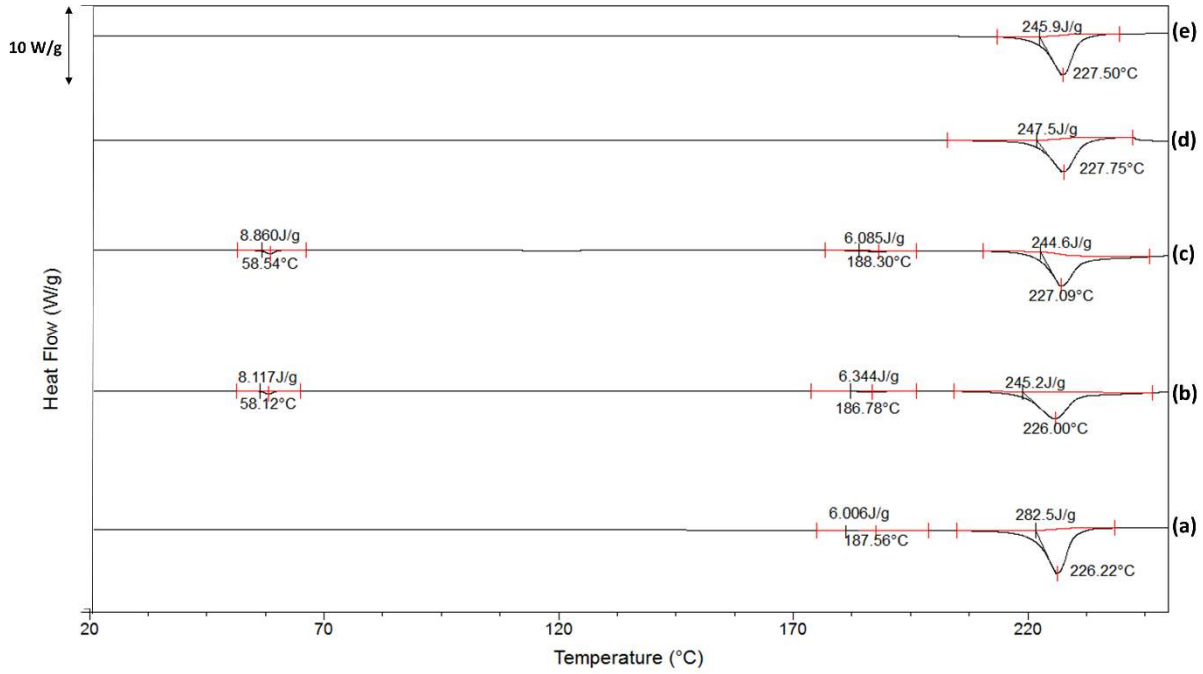

915

916 **Figure 6.** DSC thermograms of (a) physical mixture of MET and SIT in the ratio 850:63, (b)
917 physical mixture of HPC-S formulation, (c) physical mixture of HPC-A formulation, (d) melt
918 granulation of HPC-S formulation and (e) melt granulation of HPC-A formulation.

919

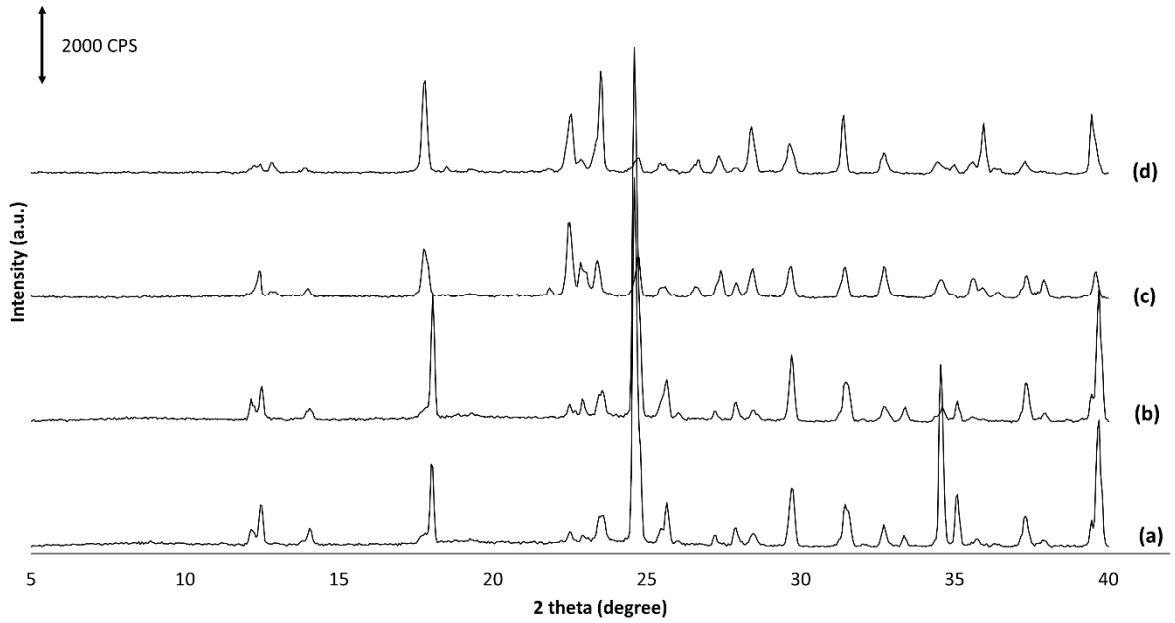

Figure 7. PXRD over the range of 5–40° 2θ: (a) physical mixture of HPC-S formulation (b) physical mixture of HPC-A formulation (c) melt granulation HPC-S formulation and (d) melt granulation HPC-A formulation.

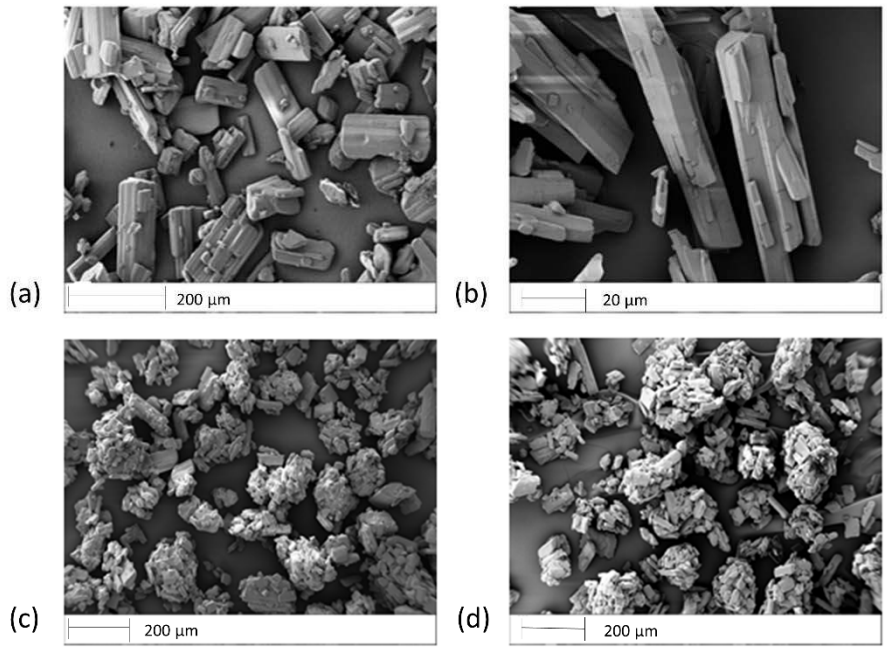

Figure 8. SEM micrographs of (a) MET raw material, (b) SIT raw material, (c) MG HPC-A formulation and (d) MG HPC-S formulation. Note the different scale bars on the figures. The scale bars on figures (a), (c) and (d) are 200 µm, while that on figure (b) is 20 µm)

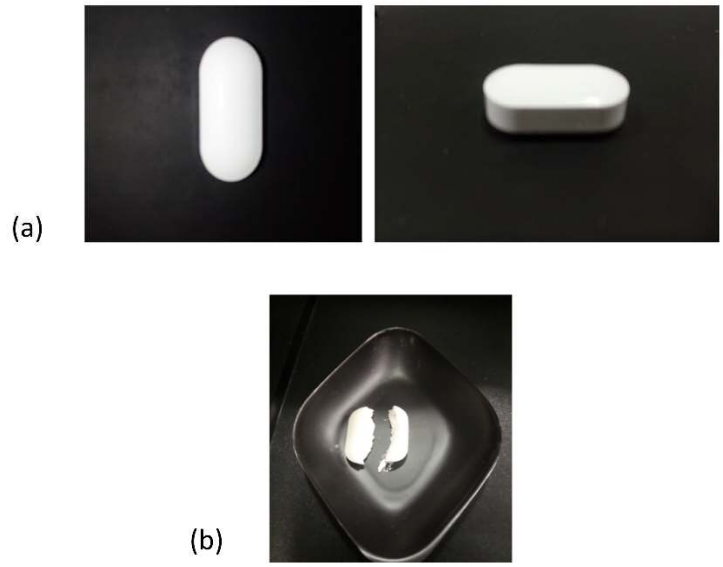

928

929 **Figure 9.** (a) Photographs of the manufactured caplets and (b) image of axial fracture of caplet
930 after hardness test.

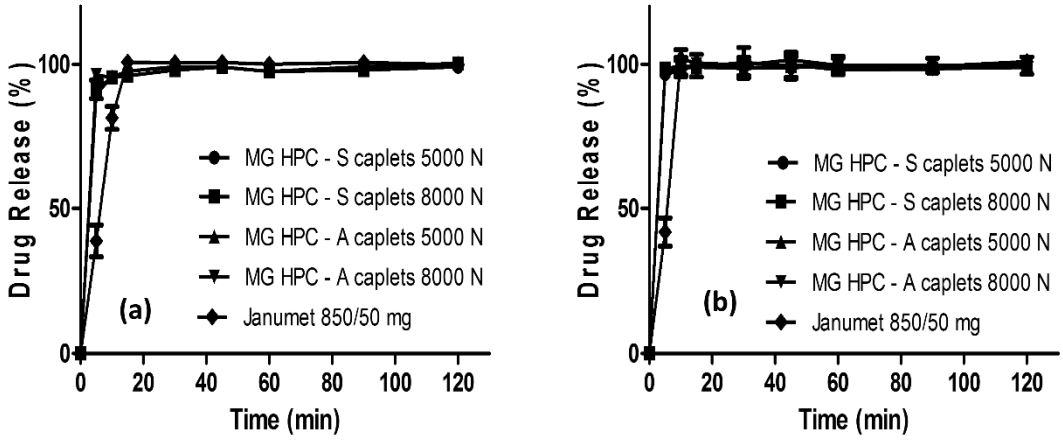

931

932 **Figure 10.** Dissolution of melt granulation (MG) caplets in pH 1.2 showing (a) MET release
933 profiles and (b) SIT release profiles. Dissolution of Janumet® also included for reference.

934 **Table I**. Physicochemical properties of HPC polymers used in the study (14–16).

	Hydroxypropoxy content (%)	Moles of substitution[a]	Molecular weight (g/mol)
HPC-A	75	3.8	1,150,000
HPC-S	65	3.0	100,000
L-HPC	11	0.2	100,000

[a]moles of substitution is the number of moles of hydroxypropyl groups per glucose unit.

Table II. Specification of Rondol 10 mm Microlab extruder.

Specification	Value	Unit
Screw diameter	10	mm
Screw speed	0~200	rpm
Profile	Co-rotating, intermeshing	-
Number of barrel heating sections	4	-
Length of each barrel section	05:01	L/D
Overall barrel length	20:01	L/D
Minimum run size	10	g
Typical wastage	<3	g
Maximum processing temperature	300	°C
Materials of construction of the barrel	High strength carbon steel	-
Cooling water requirement	1	L/min

945 **Table III**. Summary and composition and processing temperature for optimised formulations.

Proportion (% w/w) of components in MG formulation			
MET	SIT	PEG 3350	HPC-A or HPC-S
80	6.00	4.0	10.0
Processing Temperature (°C)			
Zone 3	Zone 2	Zone 1	Feed Zone
180	170	150	130

946

947 **Table IV**. Overview of particle size analysis (PSA) results (median particle size, d50) of API
948 raw materials and processed MG formulations.

Sample	**Particle size (d50) (µm)**
MET	115.08 ± 10.88
SIT	28.64 ± 0.80
MG HPC-A formulation	221.67 ± 13.80
MG HPC-S formulation	281.67 ± 55.05

949

950

951

952

953

954

Table V. Summary of flow parameters of physical mixtures (PM), manufactured melt granules (MG) and manufactured MG materials with glidant.

Sample	AIF, º	Cohesion, kPa	FF
PM MET SIT HPC-A PEG	31.45 ± 1.06	0.81 ± 0.13	5.61 ± 0.84
PM MET SIT HPC-S PEG	32.01 ± 2.55	0.84 ± 0.18	5.57 ± 0.85
MG MET SIT HPC-A PEG	32.00 ± 1.56	1.05 ± 0.13	4.74 ± 0.69
MG MET SIT HPC-S PEG	34.30 ± 1.28	0.79 ± 0.18	5.38 ± 1.32
MG MET SIT HPC-A PEG and glidant (10 % w/w)	30.45 ± 1.15	0.85 ± 0.09	5.41 ± 0.84
MG MET SIT HPC-S PEG and glidant (10 % w/w)	31.80 ± 1.73	0.74 ± 0.14	5.21 ± 0.45

Table VI. Jenike classification of flowability by flow function (FF) (52).

Flowability	No flow	Very cohesive	Cohesive	Easy flow	Free flowing
Flow function	<1	<2	<4	<10	>10

965

966

967 **Table VII**. Content assay (%) of melt granulation (MG) formulations.

Formulation	MG HPC-S formulation	MG HPC-A formulation
MET (% of max theoretical amount)	98.12 ± 0.84	98.84 ± 0.46
SIT (% of max theoretical amount)	99.14 ± 0.35	98.47 ± 0.74

968

969 **Table VIII**. Dimensions of melt granulation (MG) manufactured caplets post compression at
970 different compression forces.

Sample	MG HPC-A formulation		MG HPC-S formulation	
Compression force to form caplets (N)	5000	8000	5000	8000
L (mm)	21.39 ± 0.02	21.43 ± 0.03	21.41 ± 0.02	21.44 ± 0.02
D (mm)	10.52 ± 0.02	10.52 ± 0.02	10.52 ± 0.02	10.51 ± 0.03
t (mm)	6.32 ± 0.01	6.03 ± 0.05	6.14 ± 0.02	5.93 ± 0.03
w (mm)	3.93 ± 0.01	3.59 ± 0.08	3.58 ± 0.08	3.23 ± 0.09

971

972

973

974

975

976

977 **Table IX**. Results of the tablet hardness test for MG formulations compressed into caplets at
978 different compression forces.

Sample	**MG HPC-A formulation caplets**		**MG HPC-S formulation caplets**	
Compression force to form caplets (N)	5000	8000	5000	8000
Tensile strength of Melt Granulation products (MPa)	0.22 ± 0.01	0.31 ± 0.01	0.28 ± 0.03	0.44 ± 0.05

979

980 **Table X**. Friability test results for melt granulation caplets compressed at different
981 compression forces.

Sample	**MG HPC-A formulation caplets**		**MG HPC-S formulation caplets**	
Compression force to form caplets (N)	5000	8000	5000	8000
Friability of Melt Granulation caplets (%)	65.53 % (Fail)	81.08 % (Fail)	91.96 % (Fail)	99.25 % (Pass)

982

983

984

985

Table XI. Disintegration times of MG caplets compressed at different compression forces.

Sample	**HPC-A formulation**		**HPC-S formulation**	
Compaction force to form caplets (N)	5000	8000	5000	8000
Disintegration of Melt Granulation caplets (seconds)	70 ± 12	257 ± 55	235 ± 35	748 ± 28